

Article

Assessment of Wave Power Density Using Sea State Climate Change Initiative Database in the French Façade

Sonia Ponce de León ^{1,*}, Marco Restano ² and Jérôme Benveniste ³

¹ Centre for Marine Technology and Ocean Engineering (CENTEC), Instituto Superior Técnico, University of Lisbon, Avenida Rovisco Pais 1, 1049-001 Lisbon, Portugal

² SERCO/ESRIN, Largo Galileo Galilei, I-00044 Frascati, Italy; marco.restano@ext.esa.int

³ European Space Agency-ESRIN, Largo Galileo Galilei, I-00044 Frascati, Italy; jerome.benveniste@esa.int

* Correspondence: soniaponcedeleon@tecnico.ulisboa.pt

Abstract: This study considers assessing the wave energy potential in the French façade. The objective is to investigate the validity of satellite altimetry-based estimates of wave renewable energy potential using the homogenized multi-mission altimeter data made available by the European Space Agency Sea State Climate Change Initiative (Sea_State_cci). The empirical model of Gommenginger et al. (2003) is adopted to calculate the wave period, which is required to estimate the wave power density from both the radar altimeter's significant wave height and backscatter coefficient. The study comprises 26 years of data, from January 1992 to December 2018. In the winter season, the wave resource is abundant and higher than in other seasons. On average, the highest value is about 99,000 W/m offshore. In the coastal zone, the wave power density is also relatively high, with values of about 60,000 W/m in the North and South regions of the French Atlantic coast. The seasonal spatial distribution of the wave power density is presented to identify potential sites of interest for the development of the marine renewable energy sector and to make renewable energy supply more resilient. The analysis reveals large inter-annual and interseasonal variability in the wave resource in the French façade in the past 26 years. The study shows the feasibility of satellite altimetry-based assessments of wave renewable energy potential as a promising and powerful tool.

Keywords: renewable energy; wave power density; oceanography; Sea State Climate Change Initiative; satellite altimetry; Atlantic French façade



Citation: Ponce de León, S.; Restano, M.; Benveniste, J. Assessment of Wave Power Density Using Sea State Climate Change Initiative Database in the French Façade. *J. Mar. Sci. Eng.* **2023**, *11*, 1970. <https://doi.org/10.3390/jmse11101970>

Academic Editor: Eugen Rusu

Received: 1 September 2023

Revised: 9 October 2023

Accepted: 9 October 2023

Published: 11 October 2023



Copyright: © 2023 by the authors. Licensee MDPI, Basel, Switzerland. This article is an open access article distributed under the terms and conditions of the Creative Commons Attribution (CC BY) license (<https://creativecommons.org/licenses/by/4.0/>).

1. Introduction

Renewable energies have become a subject of broad importance, and their sources are the goal of many governments and agencies. Natural wave energy, in particular, has been identified in recent years as a solid source of energy. Harvesting energy from waves might constitute a possibility to both alleviate the energy crisis and accelerate the transition from fossil fuels.

However, the exploitation of natural wave energy is far from being a reality. The diversified principles of operation of wave energy converters (WECs), exploiting a variety of wave characteristics, have so far resulted in a lack of technology convergence [1].

Numerous past projects on wave power, like the Aguçadoura Wave Farm in Portugal (the first wave farm in the world that integrated three Pelamis devices [2,3]), resulted in failure. At present, ongoing projects from the Eco Wave Power company [4] aim at developing a smart and cost-efficient technology for turning ocean and sea waves into green electricity.

One of the key industrial challenges is to create efficient operations at sea and to improve the WEC's design to account for climate change (i.e., for potential changes in the spatio-temporal variability of the available wave power [5], where extreme sea states could be more frequent). In this regard, [1] optimized WEC's control algorithms, emphasizing that the performance is device- and wave climate dependent.

Much of the published material on wave energy assessment [6–9] has included observations from wave buoys that were sparse in specific domains (e.g., wave observations from vessels or spectral wave models forced with wind reanalysis). An attempt to assess the wave resource in the North Sea using the ESA Sea_State_cci and ERA5 data was made and reported in [10].

It is worth noting that on the French coast, some studies have been based on numerical applications, adopting spectral wave models at a high spatial resolution of 200 m to exploit and evaluate the wave power [11,12]. An interesting comparison between different spectral wave models was provided by [13], who concluded that the wave energy resource of Brittany is characterized by increased inter-annual variations. The wave energy resource in the French Atlantic coasts from a 33-year hindcast (1979–2011) was instead quantified by [14] providing information about the variability of the wave resource.

Thanks to the advantages brought by satellite altimetry data temporal and spatial resolution, studies have been developed to infer the capabilities of this data to estimate wave trends. At present, homogenized altimetry databases like the ESA Sea_State_cci [15] offer the advantage of global coverage and a large time span of 26 years to assess the wave energy resource. Among the previous efforts using satellite altimeter data, [16–20] can be mentioned. Without any doubt, satellite altimetry missions have brought a new perspective and paved the way for the ocean renewable energy assessment from space.

In addition, high-resolution synthetic aperture radar (SAR) altimetry products, e.g., from the ESA CryoSat-2 mission, processed with coastal zone algorithms such as SAMOSA+ [21,22], represent a new possibility to assess the potential of the wave energy on the coast. The SAMOSA+ algorithm, in fact, allows the recovery of a greater amount of valid coastal data, which are posted every 300 m along the satellite track. In this sense, the work of [16], based on CryoSat-2 data processed with the SAMOSA+ model over an 11-year period, assessed the wave resource in the French Atlantic coastal zone, concluding that its exploitation could be promising for the near future.

The French façade was chosen for this study because various wave energy conversion devices operate in the area. Wave energy has great potential in the coastal zone, where its conversion to electricity is most needed. As this resource has not been exploited yet as it might be, identifying the most adequate places that own the greatest potential for the installation of wave energy converters (WECs) and an efficient recuperation of the resource is essential.

This study presents satellite altimetry-based assessments of wave energy potential in the French façade using the homogenized multi-mission altimetry data of the European Space Agency Sea_State_cci database to estimate the wave power density on chosen sites along the French façade. The empirical model of [23] is used to find the wave period from the altimeter data and wave buoys. The advantage of this method is that once the wave period is known, the wave power density can be estimated only using satellite altimetry data, which provides a large spatial coverage at any other location where wave buoys are unavailable. To our knowledge, this is the first wave energy assessment in the French façade using a long time series from the 26 years of satellite altimetry data Sea_State_cci database. The high spatial resolution of the along-track wave energy density estimates is an advantage when assessing the wave energy resource over the sparse estimates that can be obtained by wave buoys, allowing us to determine the locations with the optimal conditions for harvesting wave energy.

The paper is organized as follows: Section 2 gives a brief description of the French façade, data, and methods. Section 3 is devoted to results and discussion. In this section, the temporal and spatial distribution of the wave power density over 26 years is analyzed. A seasonal analysis of the wave power density over 26 years is also reported. Moreover, locations with ideal conditions for wave harvesting along the coastal zone of the French façade are analyzed. In Section 4, some aspects of the correlation between wind and waves are discussed, as well as the variability existing in the coastal zone of the French façade. Finally, in Section 5, conclusions and recommendations are given.

2. Material and Methods

2.1. The French Façade

The French façade, located in Western Europe, is a highly energetic region being exposed to swells arriving from the Atlantic storms [12]. The continental shelf encompasses several hundred kilometers, presenting a highly variable bathymetry with a series of islands [12]. The coastline is also irregular, presenting several small islands and a coastal ledge (Figure 1). Because of the offshore and nearshore islands, some parts of the French façade are situated in the shadow side, while others are exposed to storm swells, making this region a complex scenario for wave energy recuperation decision-makers.

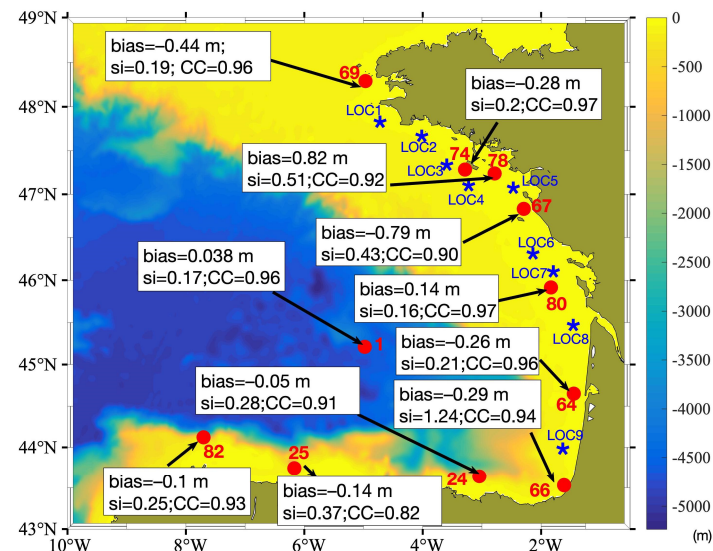


Figure 1. Study area. Bathymetry (colormap, in meters), wave buoys (red circles), and locations where the wave power density is estimated (1–9, blue stars).

Moreover, this coast, surrounded by several irregular islands, is characterized by strong tidal regimes with velocities that can reach values as high as 4 ms^{-1} near the sea surface within straits separating islands from the landmass [13]. The littoral sea state is consequently characterized by wave–current interactions, which modify the significant wave height and wave power due to the wave–current refraction and other processes inherent in the coastal steepening and breaking.

2.2. Data

The European Space Agency (ESA) “Sea_State_cci” database (version 1.1) [15,24] is adopted for the present study. The Climate Change Initiative (cci) programme was launched by the European Space Agency in 2010 to contribute to creating new climate data records (CDRs). In this context, the Sea_State_cci project was kicked off in 2018 to produce new CDRs from low-resolution mode measurements (~ 2 – 17 km resolution, dependent on sea state) provided by satellite altimetry missions. These CDRs address a specific essential climate variable (ECV), the sea state, which critically contributes to the characterization of Earth’s climate, providing a picture of climate change at a global scale.

The Sea_State_cci database is composed of ten missions encompassing the period of 1991–2018 (26 years): TOPEX, ENVISAT, ERS-1, ERS-2, GFO, SARAL/AltiKa, Jason-1, Jason-2, Jason-3, and CryoSat-2. Although many spaceborne radar altimeters adopt, or have adopted, dual-frequency schemes to derive ionospheric corrections (Ku-C or Ku-S), only Ku-band measurements are used, for consistency reasons, in deriving sea state-related estimates, these being available for all missions except SARAL/AltiKa (Ka-band).

For wave buoys located as in Figure 1, data are from the Copernicus Marine Environment Monitoring Service (CMEMS in situ TAC) database.

2.3. The Wave Power Estimation Method

2.3.1. Wave Power Density

For real seas, the wave power density (P_{wave}) per unit of wave-crest length can be estimated by (1) [25]:

$$P_{wave} = \frac{\rho g^2 H_s^2 T_e}{64\pi} \text{ (W/m)}. \tag{1}$$

In (1), ρ is the seawater density (1025 kg/m^3), g is the acceleration of gravity (9.81 m/s^2), H_s is the significant wave height (m) (the mean of the 1/3 highest waves), and T_e (seconds) is the wave energy period, defined by $m(-1)/m(0)$. It can be derived from the zero-crossing period T_z , as in Expression (2), where the 1.18 factor is valid for a JONSPWAP spectrum [26,27]:

$$T_e = 1.18 * T_z \tag{2}$$

H_s and the backscatter coefficient (σ^0) are available as satellite altimetry output products, whereas the wave period T_z has to be estimated.

2.3.2. Empirical Estimation of T_z

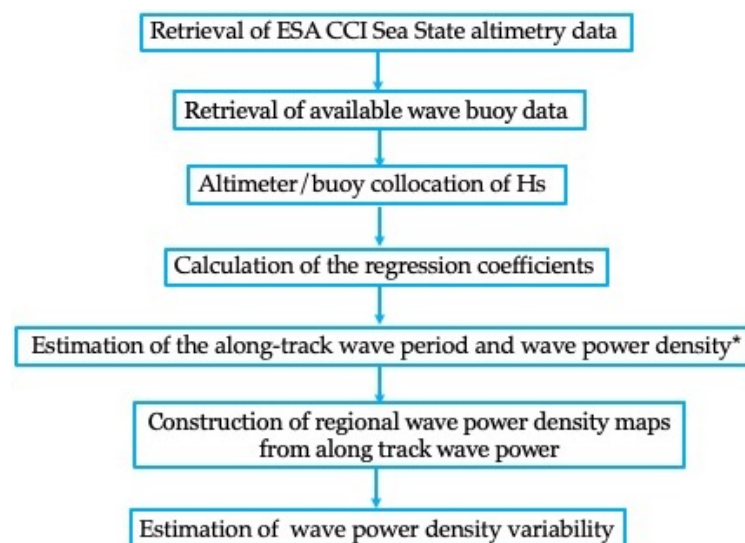
The empirical model developed in [23] is used to estimate the wave period T_z (3), which is required to estimate the wave power density from the Ku-band radar altimeter significant wave height and the radar backscatter coefficient.

The estimation method uses a simple linear relationship between the variable $X = (\sigma^0 H_s^2)^{0.25}$ and T_z :

$$T_z = a * X + b \tag{3}$$

The regression coefficients (a and b) of (3) are computed from values of X derived from the altimeter measurements and from values of T_z derived from buoys.

To obtain the (X, T_z) pairs, the altimeter and buoy measurements must be collocated. The collocation is performed by computing the average of H_s and σ^0 of the satellite observations that are at less than 100 km from the buoy location and whose observation time is within a 45-min window around the buoy datum time. In addition, only the satellite observations farther than 25 km from land and whose quality flag is set to “good” are used to avoid bad data and land contamination of altimetry estimates. The processing steps to obtain the wave power estimates are depicted in Scheme 1.



Scheme 1. Processing steps to obtain the wave power estimates. * The estimation of T_e and P_{wave} can also be made for a specific site by estimating H_s and σ^0 for the specific site and using the regression coefficients “ a ” and “ b ” from the nearest buoy (or by interpolating “ a ” and “ b ” from several buoys).

The empirical method is validated with wave buoys along the coastal zone of the Atlantic French façade. Table 1 shows the fit between wave buoy data and altimetry data, and the regression coefficients, respectively. The scatter plot for the H_s and the wave power density is shown in Figure 2 for the wave buoy 64. A good agreement was obtained, as can be seen from the statistical coefficients shown in Figure 2, where the correlation coefficient reached 0.95. In addition, the empirical method used to estimate the wave period was adopted and verified by several authors [16,17,23,28] for different sea state conditions.

Table 1. Regression coefficients (a and b).

Buoys	Regression Coefficients
78 (2010–2018)	a = 1.4302; b = 1.6812
67 (2005–2018)	a = 1.1129; b = 2.672
69 (2008–2018)	a = 1.5917; b = 2.0901
64 (2004–2018)	a = 1.713; b = 2.0250
74 (2011–2018)	a = 1.6616; b = 1.7943
80 (2014–2018)	a = 2.216; b = 0.571
66 (2004–2018)	a = 2.210; b = 1.3477
1 (1998–2018)	a = 1.8834; b = 1.8863
24 (1990–2018)	a = 1.9861; b = 1.1065
25 (1996–2018)	a = 1.7340; b = 1.649
82 (1997–2018)	a = 1.6790; b = 1.517

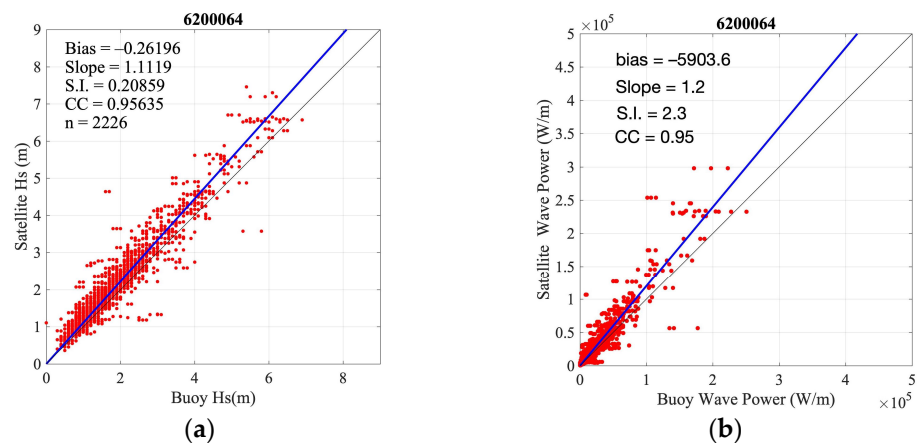


Figure 2. Scatter plots for the significant wave height (H_s) (a) and the wave power density (b) for coastal buoy 64.

The value of the statistical fit coefficients varied with the location of the buoy (Figure 1). The bias was larger for buoys located in the northern part of the domain, whereas the scatter index was larger for locations closer to land. The correlation coefficient was higher than 0.90, except for buoy 25. In conclusion, the location of the buoys appeared to have an effect on the agreement between satellite and buoy data. This can be related to the sheltering effect of the land on the wave fields and also to the degradation of the satellite data as the altimeter approaches the land very closely, although we recall that land contamination on the measurements is controlled by: (1) removing measurements flagged as bad, and (2) using a large enough radius for the satellite-buoy collocation.

2.3.3. Coefficients of Variability

To evaluate the temporal variability of the wave energy on the French façade, different coefficients are estimated. The coefficient of variation (COV), the seasonal variability coefficient (SVC), the monthly variability index (MVI), and the annual variability index (AVI) are estimated following expressions from [25].

The amount of variability in relation to the mean is obtained by dividing the standard deviation (σ) by the mean (\bar{P}). This is expressed by the coefficient of variation (COV):

$$\text{COV} = \frac{\sigma}{\bar{P}}, \tag{4}$$

The seasonal variability index (SVI) provides instead the variability of the wave power resource:

$$\text{SVI} = \frac{P_{max} - P_{min}}{\bar{P}}, \tag{5}$$

where P_{max} is the mean wave power of the most energetic season, P_{min} is the mean wave power of the less energetic season, and \bar{P} is the yearly mean estimated over the 26-year period.

The monthly variability index can be estimated by:

$$\text{MVI} = \frac{P_{Mmax} - P_{Mmin}}{\bar{P}}, \tag{6}$$

where P_{Mmax} is the mean wave power density of the most energetic month and P_{Mmin} is the mean wave power density of the less energetic month.

The annual variability index is calculated as:

$$\text{AVI} = \frac{P_{Amax} - P_{Amin}}{\bar{P}}. \tag{7}$$

3. Results and Discussion

Seasonal Analysis

According to the 26-year mean wave power density map (Figure 3), the maximum value of the wave power density near the coast, above 45.5° North, was about 15,000 W/m. The mean wave power density was higher below this latitude and near the coast, ranging from 20,000 W/m to 30,000 W/m. These values align with [11], who reported 40,000 W/m offshore and less than 15,000 W/m in coastal zones. Such values were obtained from high-resolution simulations performed by relying on the phase-averaged spectral wave over a time span of 8 years (between 2004 and 2011).

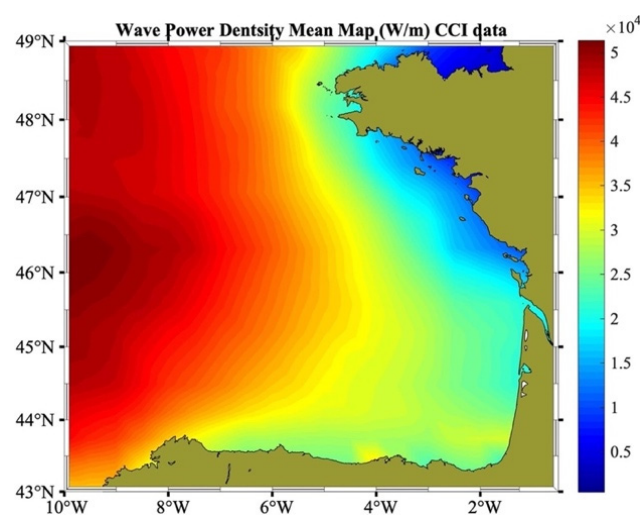


Figure 3. Mean wave power density map (W/m) for 1992–2018.

The mean wave power density was higher offshore, reaching a maximum value of 50,000 W/m. A more detailed similar conclusion can be drawn from the mean wave power density map computed with a higher grid cell of 1.3 km (Figure 4), where it is possible to distinguish the tracks of each of the ten satellites that compose the Sea State_cci database.

By zooming into the 26-year mean wave power map (Figure 5), it can be better appreciated where the highest wave resource is located along the satellite tracks. However, Figure 5 also shows many areas where observations were not available. Consequently, potential areas of utmost importance for the installation of WEC machines cannot be inferred with the adopted Sea State_cci dataset. High-resolution SAR mode measurements from CryoSat-2, Sentinel-3, and Sentinel-6 altimetry instruments (~300 m resolution in the along-track direction, independent from sea state), processed with coastal zone-dedicated algorithms like SAMOSA+ [16,21,22], could be the turning point for future renewable energy assessments. These should also consider fully focused synthetic aperture radar (FF-SAR) [29] data (providing a resolution up to ~0.5 m in the along-track direction, independent from the sea state).

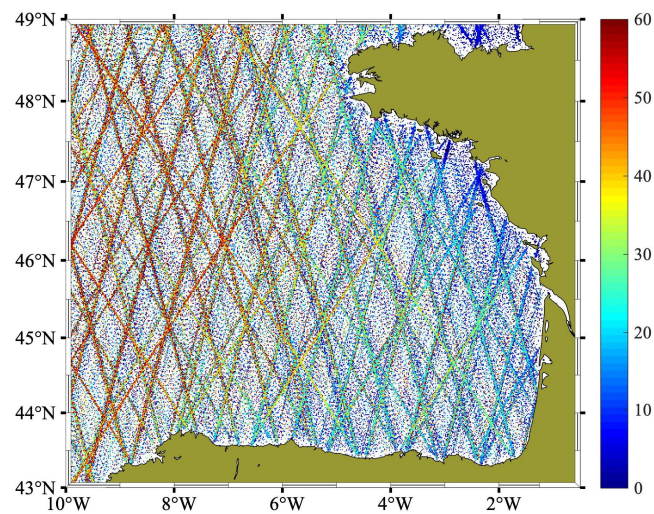


Figure 4. Along-track mean wave power density map (kW/m) for 1992–2018.

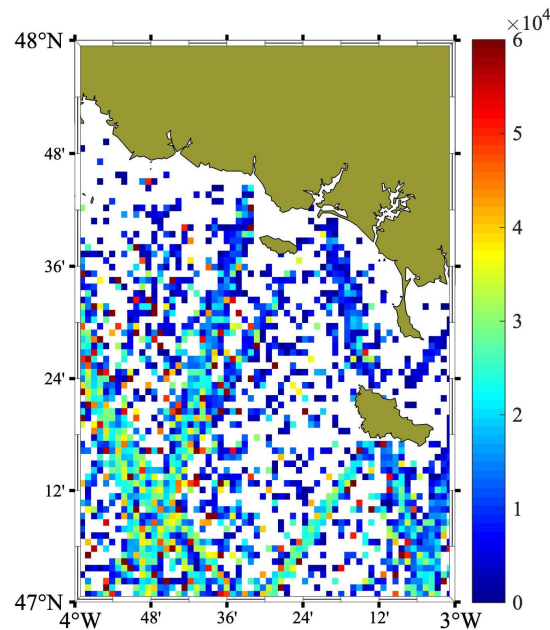


Figure 5. Mean wave power density map (W/m) for 1992–2018. Zoom of the coastal section.

From the 26-year seasonal mean wave power density maps (Figure 6), it can be seen that the highest values of mean wave power density were located offshore. Moreover, because of the low spatial resolution of the Sea_State_cci altimetry data, coastal zone results must be taken with caution.

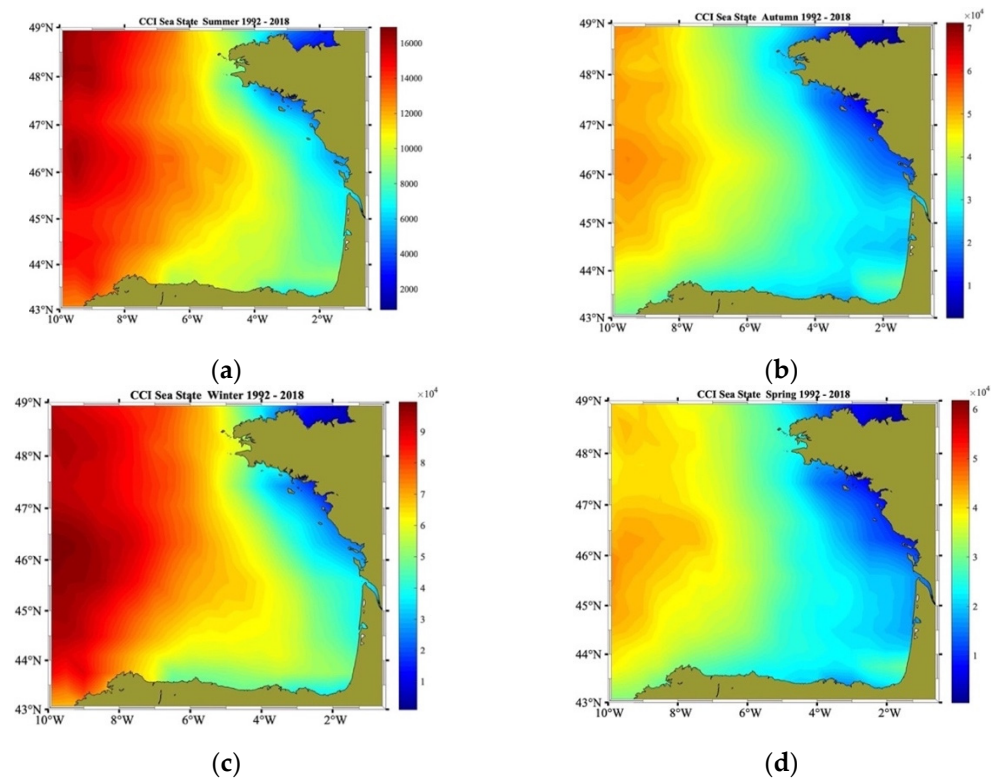


Figure 6. Seasonal distribution of mean wave power density (W/m) for 1992–2018. Summer (a), autumn (b), winter (c), and spring (d).

As expected, the summer (Figure 6a) was less attractive in terms of wave energy resources. A low wave power density was reported due to the relatively calm sea state conditions (the highest values may reach $16,000 W/m$ offshore). Along the coast, in the North and the South of the French façade, relatively high values ($10,000 W/m$) could be found. However, in the rest of the coastal zone, values were way lower, in the range of 4000 to $6000 W/m$.

Autumn and spring (Figure 6b,d) were very similar regarding the spatial distribution and magnitude of the wave energy resource. The highest values oscillated between $70,000 W/m$ (autumn) and $60,000 W/m$ (spring) offshore. Along the coasts, the highest wave power density was found in the South in autumn ($35,000 W/m$); however, in spring, the highest wave resource was found in both the North and South of the French façade ($35,000 W/m$).

The winter season (Figure 6c), as expected, had the highest mean wave energy. On average, this amounted to about $99,000 W/m$, recorded offshore between 6° – $10^{\circ} W$.

In the coastal zone, the wave power density was relatively high in the North and South of the French façade, with values around $60,000 W/m$. According to the results, near the islands and very near to the coast, the wave energy resource was the lowest; on average, the wave power density was about $20,000 W/m$ in winter in the region between $48^{\circ} N$ – $46^{\circ} N$ (Figure 6c).

For the period of 1979–2011, [14] reported that in the winter season, the maximum wave power was around $40,000 W/m$ and that autumn and spring had similar maximum values of $15,000 W/m$. As expected, the summer had the lowest wave power with values below $10,000 W/m$. In our study, which focused on a different period (1992–2018) and was based on satellite altimetry observations, relatively high values were obtained: winter showed a maximum value of the wave power density of about $100,000 W/m$, autumn's maximum value resulted in $70,000 W/m$, spring showed a similar value as in autumn: $60,000 W/m$ and in summer the maximum value was $16,000 W/m$, as shown in Figure 6.

To better understand the spatial distribution of the wave power density, a monthly analysis was carried out. Offshore, the wave resource was much more abundant from November to February (Figure 7, top panels), which are precisely the winter months in which WEC operations and wave energy harvesting from the ocean is more challenging because of the harsh sea state conditions. In addition, the region of high wave energy is far from the coasts. During these months, the wave power density was higher than 80,000 W/m: in November and December, the average wave power density was about 82,000 W/m and 90,000 W/m, respectively. In October, the wave power density was about 60,000 W/m. September was characterized by lower values of about 30,000 W/m. As predicted by the mean maps (Figure 6), the wave energy resource does not appear to be abundant during spring and summer, being 40,000 W/m in April, 30,000 W/m in May, 22,500 W/m in June, 14,000 in July, and 16,000 W/m in August, respectively.

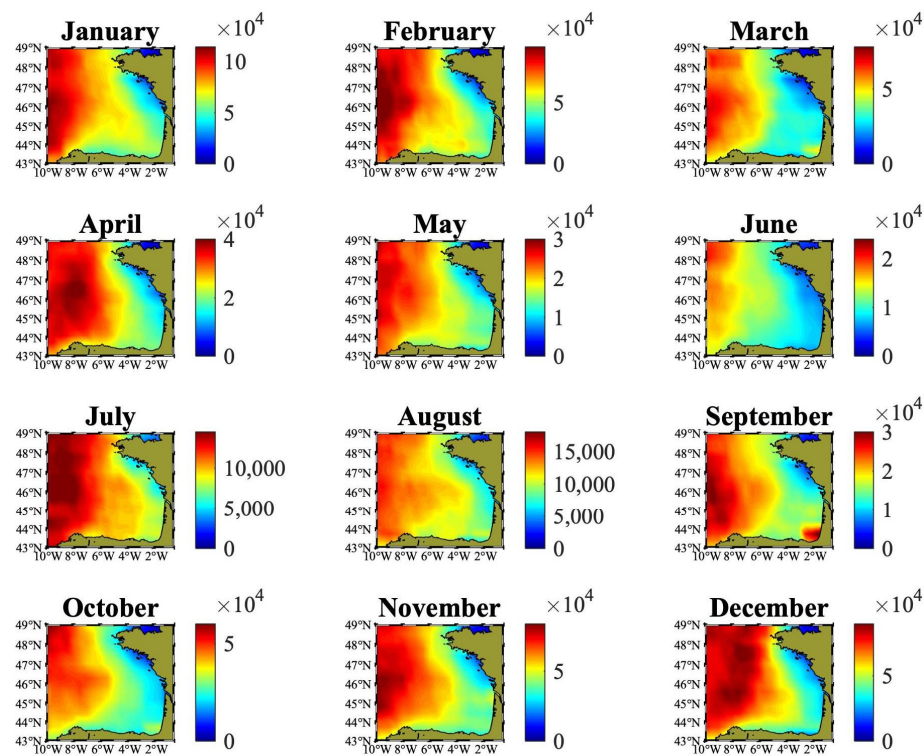


Figure 7. Monthly mean wave power density (W/m) maps over 26 years (1992–2018).

Nearshore, in winter, the mean wave power density was high in the North and South of the French façade. The average value for both January and February was around 60,000 W/m. In March, the value reached 50,000 W/m, and from April, the wave power resource started decreasing until it reached 20,000 W/m in May.

In July, the wave power decreased everywhere along the coastal sectors, reaching 6000 W/m except for the areas surrounding the islands, where the wave resource was lower than 5000 W/m. These quantities were similar for the rest of the months (August, September, and October). In the South part below 44° N, the wave resource was relatively high, as in September, with 30,000 W/m.

From November, the wave power density increased to 55,000 W/m in the north and close to the estuary of the Garonne River (45° N). In December, along the coastal sector, between 48° N and 44.5° N, the wave power density was not abundant (Figure 7, bottom right), with values below 30,000 W/m. Again, coastal results need to be taken with caution since satellite altimetry data accuracy at the coast is sensitive to the presence of land in the radar footprint; this is why, in this study, results are valid up to a certain distance from the coast after filtering out the contaminated data (Section 3).

In summary, the optimal months for wave energy extraction nearshore were November, December, January, and February in the North and South of the French façade. Offshore, the mean wave power density was higher, but the resource extraction is more difficult to realize.

For each of the locations (1–9) of Figure 1, the monthly wave power density charts were also estimated (Figure 8). Therefore, It is possible to identify places in the French façade that would be optimal for wave energy conversion activities. The ideal conditions for wave energy harvesting nearshore seem to exist in the region between 47.25° N and 46.0° N, where the resource is relatively abundant, and sea state conditions are not harsh enough to affect the operation of WECs. The ideal locations are LOC 4, 5, 6, and 7. Here, the wave power reaches relatively high values of around 45,486 W/m and 30,190 W/m in winter and autumn, respectively (Figure 8j–l).

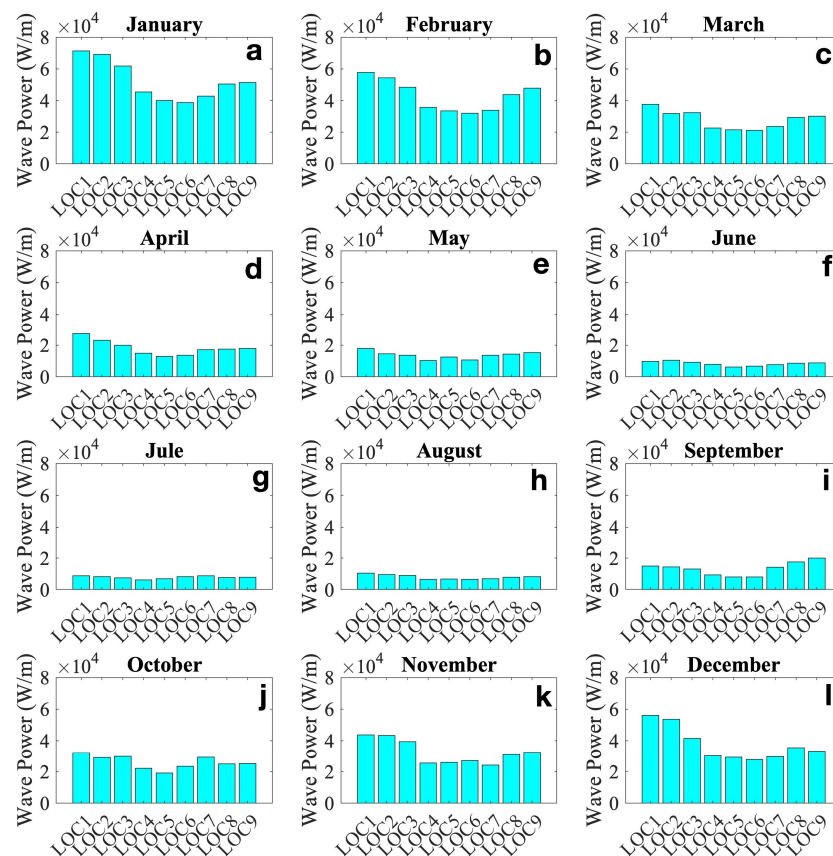


Figure 8. Monthly wave power density charts over 26 years (1992–2018). January (a), February (b), March (c), April (d), May (e), June (f), July (g), August (h), September (i), October (j), November (k), December (l).

In April, locations LOC1, LOC2, and LOC3 would also be interesting places to harvest the wave energy resource, with a wave power that can be higher than 20,000 W/m (panel d). September is also a favorable month, but only in the South (LOC9), where the wave power is higher than 20,000 W/m.

Locations 3, 4, 6, and 7 (Figure 8) are the ideal places where wave harvesting could be optimal, because both the wave energy and the variability of the resource are relatively high.

The best season for wave power harvesting at the mentioned locations could be autumn, when the wave resource is guaranteed and the operation of WECs is not dangerous.

4. Variability

Essential information for transforming wind and marine energy into electricity is the knowledge of the local correlation between the wind and waves. To understand how both resources are correlated along the French façade, the correlation was estimated using the Sea_State_cci data for nine locations (ordered from North to South) chosen along the coast (see locations marked with stars in Figure 1). From Figure 9, locations 4, 5, and 6 appeared relatively uncorrelated. The optimal condition would be to have low wave energy variability in areas where waves and wind are relatively uncorrelated. The different bars represent the various locations chosen for the study along the French façade.

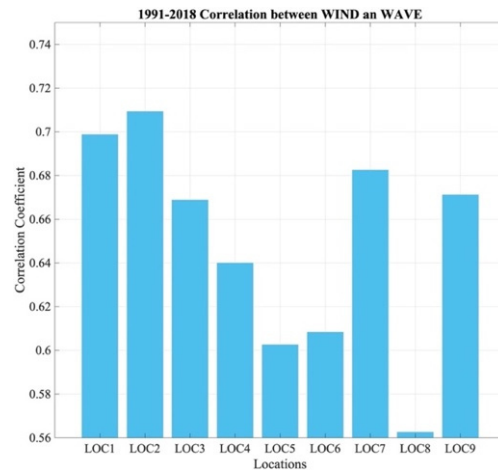


Figure 9. Local correlation between wind and waves estimated from Sea State_cci data at the nine chosen locations (Figure 1) for 1992–2018.

The highest correlation (Figure 9) between wind and waves was found in the north of the French façade between 48.5° and 47° North, where locations 1 and 2 are located. In addition, the ideal conditions for installing combined WECs (wind and waves) can be found in coastal regions at locations 4, 5, and 6, where operating companies are harvesting the wave energy. In these three locations, wind and waves seem relatively uncorrelated, meaning that although the wind resource does not exist, it is always expected to count on the wave resource from Atlantic storms. Another factor that could affect these locations is the variability of the tidal current, which is out of scope in the present study.

The lowest correlation between wind and waves was found in front of the Garonne River mouth (location 8), where it could be affected by the discharge of the river (Figure 9). Locations 7 and 9 also presented a high correlation between wind and waves.

However, not all is about correlations, but also about variability, which is an additional factor to consider in installing combined WECs. The variability of the wind/wave power has an uncontrollable nature, which affects the effectiveness of WECs [30]. The seasonal variability coefficient (SVC) estimated at each location showed that no correspondence exists between the seasonal wind variability indicator (Figure 10a) and the seasonal wave variability indicator (Figure 10b). From the wind indicator (Figure 10a), the largest variability was found in the southern part below 46.5° N (locations 6, 7, 8, and 9), whereas the lowest variability is found in the northern part (locations 3, 4, and 5).

In general, the wind seasonal variability indicator was higher than the wave seasonal variability indicator. The latter, in the northern part of the French façade, was comparable to the wind index for locations 1 and 2 (in the north) and locations 6 and 7. Locations 4, 5, and 6 presented the highest SVC for waves, which could be associated with a strong wave–current interaction in this region.

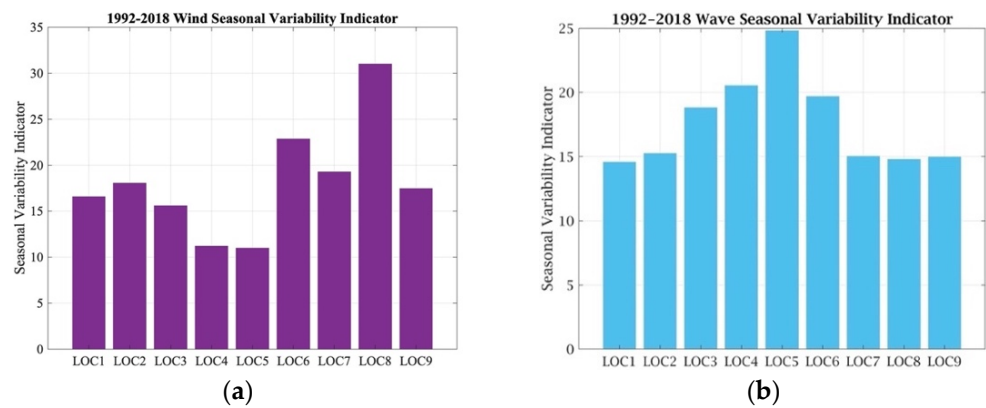


Figure 10. Seasonal variability indices estimated from the Sea State_cci data at the nine chosen locations (Figure 1) for 1992–2018. (a) wind, (b) waves.

To better understand the wave power density availability and how it varies seasonally and yearly, the spatial distribution of different statistical variability indices (COV, SVC, MVI, AVI) was estimated. As mentioned earlier, variability is an essential factor for WEC installation. A moderate wave energy flux is more suitable than a high one, as the WEC efficiency may be reduced under more severe sea state conditions. The French façade revealed substantial inter-annual and interseasonal variability of the resource during winter, as indicated by the 26-year variability indices estimated from the observed wave power density.

The four statistical variability indices for the wave power density are shown in Figure 11. Values higher than 1.2 indicate substantial variability in the wave resource [31]. As values above 1.5 were returned by all the indices, considerable temporal variability was found almost everywhere. Nearshore, the lowest temporal variability indices were sporadically found, having lower energy.

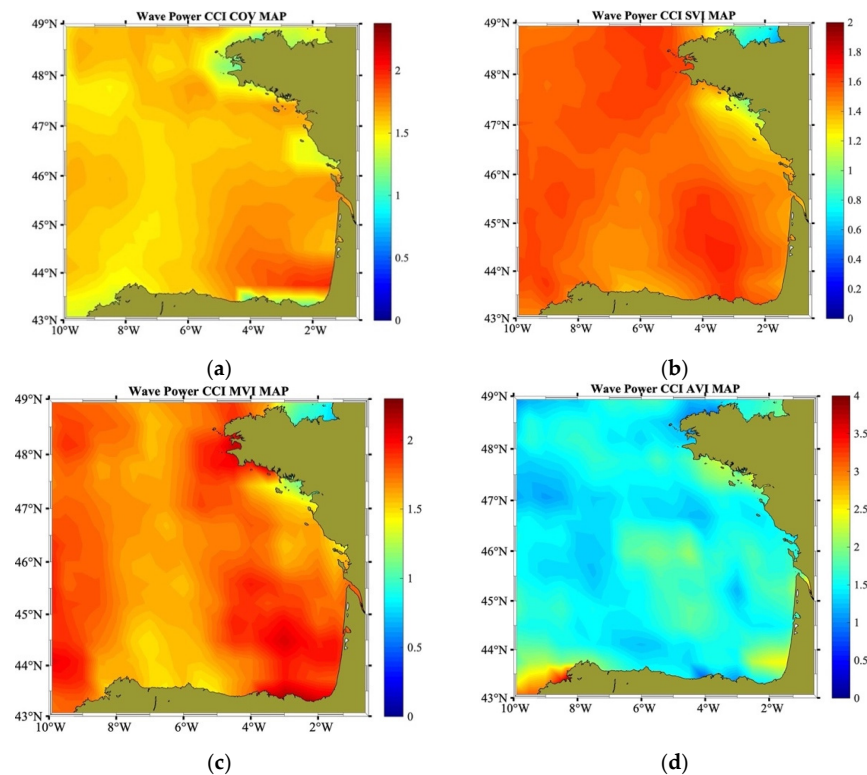


Figure 11. Wave power variability indices: coefficient of variation (COV) (a), seasonal variability index (SVI) (b), monthly Variability index (MVI) (c), and annual variability index (AVI) (d).

In particular, the COV showed that the variability was high in the south of the coastal zone with values higher than 2 (Figure 11a). The SVI (Figure 11b) showed large values for almost the whole domain except the coastal zone between 47.5° and 46.8° N, between islands and continental France, where the SVI was lower than 1 (low seasonal variability). The MVI (Figure 11c) showed that the study region had a high monthly variability since the values were higher than 1.2.

The AVI shows that the French façade coastal zone was subject to high variability, as seen in Figure 11d. In particular, the highest annual variability was found on the South coast (below 44.25° N) and in the region of islands between 47° N and 47.85° N, where the AVI reached a value of 2.5.

5. Conclusions

The obtained results reveal a substantial inter-annual and interseasonal variability in the wave energy resource in the French façade, as the variability indices estimated from the 26-year wave power density data demonstrate. The study locations show some correspondence between variability and mean wave power, which is relevant for the marine renewable energy strategy of any jurisdiction.

The optimal conditions for harvesting wave energy are found at locations 3, 4, 6, and 7 (Figure 1), which appear characterized by a relatively high wave power density and variability of the wave energy resource.

The results obtained using ESA Sea_State_cci data show the feasibility of satellite altimetry-based assessments of wave renewable energy potential as a promising, powerful tool. The global coverage and the provision of significant wave height measurements, together with the capability of estimating wave periods, demonstrate that satellite altimeters are useful systems for investigating site-specific wave energy potential.

However, valid coastal data closer to land are required to improve the analyses. In this regard, Sentinel-3A/B and CryoSat-2 SAR altimeter data, processed with coastal algorithms like the SAMOSA+ model, are expected to play a key role in future investigations. The ESA Altimetry Virtual Lab hosted on Earth Console[®] can provide this advanced data to the community.

The presented methodology will be extended to other coastal locations worldwide. Since the altimeter record is global and already covers several decades, the application of this method is limited mostly by the availability of buoy data, which is generally limited to locations close to land. However, existing WEC prototypes are also mostly designed to be installed close to land, so the lack of offshore buoy data is not a hindrance to the application of the method in coastal locations. In conclusion, it is possible to extend the presented methodology to other coastal locations worldwide if buoy data is available.

Author Contributions: Conceptualization, methodology, validation, programming, formal analysis, investigation, writing—original draft preparation, S.P.d.L.; investigation, review, and editing, M.R.; investigation, supervision, review, editing, and funding acquisition, J.B. All authors have read and agreed to the published version of the manuscript.

Funding: This research was funded by the European Space Agency Earth Observation Visiting Scientist program (FutureEO) in ESA-ESRIN, where the first author was enrolled in 2022.

Data Availability Statement: Data are freely available at the European Space Agency: <https://climate.esa.int/en/projects/sea-state/data/> (access date: 1 June 2022); ESA Altimetry Virtual Lab hosted in the Earth Console[®]: <https://eo4society.esa.int/resources/earthconsole-altimetry-virtual-lab/> (access date: 4 August 2022); Copernicus Marine Environment Monitoring Service (CMEMS in situ TAC) database: <http://www.marineinsitu.eu/> (access date: 3 May 2022).

Acknowledgments: The first author acknowledges heartedly Jérôme Benveniste, who encouraged her to apply for a Visiting Scientist stay at ESA. She also acknowledges the support of the European Space Agency and the Visiting Scientist program. This work also contributes to the Strategic Research Plan of the Centre for Marine Technology and Ocean Engineering (CENTEC), which is financed by

the Portuguese Foundation for Science and Technology (Fundação para a Ciência e Tecnologia—FCT) under UIDB/UIDP/00134/2020.

Conflicts of Interest: The authors declare no conflict of interest.

References

- Peña-Sanchez, Y.; García-Violini, D.; Ringwood, J.V. Control co-design of power take-off parameters for wave energy systems. *IFAC-Pap.* **2022**, *55*, 311–316. [[CrossRef](#)]
- Guillou, N.; Lavidas, G.; Chapalain, G. Wave Energy Resource Assessment for Exploitation—A Review. *J. Mar. Sci. Eng.* **2020**, *8*, 705. [[CrossRef](#)]
- Henderson, R. Design, simulation, and testing of a novel hydraulic power take-off system for the Pelamis wave energy converter. *Renew. Energy* **2006**, *31*, 271–283. [[CrossRef](#)]
- Eco Wave Power. Available online: <https://www.ecowavepower.com/future-projects/> (accessed on 7 September 2020).
- Reguero, B.; Losada, I.J.; Mendez, J.F. A recent increase in global wave power as a consequence of oceanic warming. *Nat. Commun.* **2019**, *10*, 205. [[CrossRef](#)] [[PubMed](#)]
- Amarouche, K.; Akpınar, A.; El Islam Bachari, N.; Houma, F. Wave energy resource assessment along the Algerian coast based on 39-year wave hindcast. *Renew. Energy* **2020**, *153*, 840–860. [[CrossRef](#)]
- Silva, D.; Rusu, E.; Guedes Soares, C. Evaluation of the expected power output of wave energy converters in the north of the Portuguese nearshore. In *Progress in Renewable Energies Offshore*; Guedes Soares, C., Ed.; Taylor & Francis Group: London, UK, 2016; pp. 875–882.
- Silva, D.; Martinho, P.; Guedes Soares, C. Wave energy distribution along the Portuguese continental coast based on a thirty three years hindcast. *Renew. Energy* **2018**, *127*, 1064–1075. [[CrossRef](#)]
- Ponce de León, S.; Orfila, A.; Simarro, G. Wave energy in the Balearic Sea. Evolution from a 29 years spectral wave hindcast. *Renew. Energy* **2016**, *82*, 1192–1200. [[CrossRef](#)]
- Rusu, L.; Rusu, E. Evaluation of the Worldwide Wave Energy Distribution Based on ERA5 Data and Altimeter Measurements. *Energies* **2021**, *14*, 394. [[CrossRef](#)]
- Guillou, N.; Chapalain, G. Numerical Modelling of Nearshore Wave Energy Resource in the Sea of Iroise. *Renew. Energy* **2015**, *83*, 942–953. [[CrossRef](#)]
- Guillou, N.; Lavidas, G.; Kamranzad, B. Wave Energy in Brittany (France)—Resource Assessment and WEC Performances. *Sustainability* **2023**, *15*, 1725. [[CrossRef](#)]
- Guillou, N.; Neill, S.P.; Thiébot, J. Spatio-Temporal Variability of Tidal-Stream Energy in North-Western Europe. *Phil. Trans. R. Soc. A* **2020**, *378*, 20190493. [[CrossRef](#)] [[PubMed](#)]
- Goncalves, M.; Martinho, P.; Guedes Soares, C. A 33-year hindcast on wave energy assessment in the western French coast. *Energy* **2018**, *165*, 790–801. [[CrossRef](#)]
- Dodet, G.; Piolle, J.-F.; Quilfen, Y.; Abdalla, S.; Accensi, M.; Arduin, F.; Ash, E.; Bidlot, J.-R.; Gommenginger, C.; Marechal, G.; et al. The Sea State CCI dataset v1: Towards a sea state climate data record based on satellite observations. *Earth Syst. Sci. Data* **2020**, *12*, 1929–1951. [[CrossRef](#)]
- Ponce de León, S.; Restano Benveniste, J.M. Assessment of wave power in the French façade inferred from high-resolution altimetry. *Remote Sens.* **2023**. *in preparation*.
- Ponce de León, S.; Bettencourt, J.; Ringwood, J.V.; Benveniste, J. Assessment of combined wind and wave energy in European coastal waters using satellite altimetry. *Appl. Ocean. Res.* **2023**. *under review*.
- Rusu, E.; Rusu, L. An evaluation of the wave energy resources in the proximity of the wind farms operating in the North Sea, 438. *Energy Rep.* **2021**, *7*, 19–27. [[CrossRef](#)]
- Idris, N.H. Wave energy resource assessment with improved satellite altimetry data over the Malaysian coastal sea. *Arab. J. Geosci.* **2019**, *12*, 484. [[CrossRef](#)]
- Uti, M.N.; Din, A.H.M.; Yaakob, O. Significant wave height assessment using multi mission satellite altimeter over Malaysian seas. *IOP Conf. Ser. Earth Environ. Sci.* **2018**, *169*, 012025. [[CrossRef](#)]
- Dinardo, S. Techniques and Applications for Satellite SAR Altimetry over Water, Land and Ice. Ph.D. Thesis, Technische Universität, Darmstadt, Germany, 2020. Volume 56, ISBN 978-3-935631-45-7. [[CrossRef](#)]
- Dinardo, S.; Fenoglio-Marc, L.; Buchhaupt, C.; Becker, M.; Scharroo, R.; Fernandes, M.J.; Benveniste, J. Coastal SAR and PLRM altimetry in German Bight and West Baltic sea. *Adv. Space Res.* **2018**, *62*, 1371–1404. [[CrossRef](#)]
- Gommenginger, C.P.; Srokosz, M.A.; Challenor, P.G.; Cotton, P.D. Measuring ocean wave period with satellite altimeters: A simple empirical model. *Geophys. Res. Lett.* **2003**, *30*, 2150. [[CrossRef](#)]
- Abdalla, S.; Kolahchi, A.A.; Ablain, M.; Adusumilli, S.; Bhowmick, S.A.; Alou-Font, E.; Amarouche, L.; Andersen, O.B.; Antich, H.; Aouf, L.; et al. Altimetry for the future: Building on 25 years of progress. *Adv. Space Res.* **2021**, *68*, 319–363. [[CrossRef](#)]
- Ringwood, J.V.; Brandle, G. A new world map for wave power with a focus on variability. In Proceedings of the 11th European Wave and Tidal Energy Conference, Nantes, France, 6–11 September 2015; Available online: https://mural.maynoothuniversity.ie/6682/1/JR_new%20world%20map.pdf (accessed on 16 December 2022).
- Cahill, B.; Lewis, T. *Wave Periods and the Calculation of Wave Power*; Virginia Tech: Blacksburg, VA, USA, 2014; p. 46259438.

27. Hasselmann, K.; Barnett, T.P.; Bouws, E.; Carlson, H.; Cartwright, D.E.; Enke, K.; Ewing, J.A.; Gienapp, A.; Hasselmann, D.E.; Kruseman, P.; et al. *Measurements of Wind-Wave Growth and Swell Decay during the Joint North Sea Wave Project (JONSWAP)*; Deutsches Hydrographisches Institut: Hamburg, Germany, 1973.
28. Amiruddin; Ribal, A.; Khaeruddin; Thamrin, S.A. A 10-year wave energy resource assessment and trends of Indonesia based on satellite 436 observations. *Acta Oceanol. Sin.* **2019**, *38*, 86–93. [[CrossRef](#)]
29. Schlembach, F.; Ehlers, F.; Kleinherenbrink, M.; Passaro, M.; Dettmering, D.; Seitz, F.; Slobbe, C. Benefits of fully focused SAR altimetry to coastal wave height estimates: A case study in the North Sea. *Remote Sens. Environ.* **2023**, *289*, 113517. [[CrossRef](#)]
30. Fusco, F.; Nolan, G.; Ringwood, J. Variability reduction through optimal combination of wind/waves resources—An Irish case study. *Energy* **2010**, *35*, 310–325. [[CrossRef](#)]
31. Sierra, J.P.; White, A.; Mosso, C.; Mestres, M. Assessment of the intra-annual and inter-annual variability of the wave energy resource in the Bay of Biscay (France). *Energy* **2017**, *141*, 853–868. [[CrossRef](#)]

Disclaimer/Publisher’s Note: The statements, opinions and data contained in all publications are solely those of the individual author(s) and contributor(s) and not of MDPI and/or the editor(s). MDPI and/or the editor(s) disclaim responsibility for any injury to people or property resulting from any ideas, methods, instructions or products referred to in the content.